Desalination and Water Treatment
www.deswater.com

doi: 10.1080/19443994.2013.778796

51 (2013) 7509–7522
December

Taylor & Francis
Taylor & Francis Group

The accuracy of the stagnant film equation in the study of electrophoretic migration of solutes near an ultrafiltration membrane—a numerical study

S.I.S. Pinto*, J.M. Miranda, J.B.L.M. Campos

Centro de Estudos de Fenómenos de Transporte, Departamento de Engenharia Química, Faculdade de Engenharia da Universidade do Porto, Rua Dr. Roberto Frias s/n, 4200-465 Porto, Portugal
Tel. +351 225081692; Fax: +351 225081449; email: spinto@fe.up.pt

Received 15 November 2012; Accepted 18 February 2013

ABSTRACT

In membrane separation processes, the film equation is frequently used since it is a fast and easy way to predict the permeate velocity. In this work, the applicability of the film equation, based on a convective–diffusive–electrophoretic migration model (CDE), is evaluated using an in-house code. CDE model accounts for the transport of charged solutes in the boundary layer over a charged membrane. Two versions of the film equation were developed: CDE I—non-linear electric potential and total rejection of components; CDE II—uniform electric field and transmission of components through the membrane. The Sherwood number profiles, along the membrane length, for bovine serum albumin and lysozyme were determined by film equations. The permeate velocities, concentrations and rejection coefficients, obtained by solving numerically the conservative equations, were used as input to film equations. The Sherwood number profiles, determined by CDE I, are independent of the electric potential at the membrane surface, for low values of electric potential. The Sherwood number profiles, determined by CDE II, are independent of the electric field, for low values of electric field. In these ranges, Sherwood number profiles are identical to those in an impermeable cell and the film equation can be used to make accurate predictions.

Keywords: Film equation; Convective–diffusive–electrophoretic migration model; Mass transport; Protein separation; Computational fluid dynamics

1. Introduction

Numerical and analytical methods have been used to predict the permeate velocity in membrane separation cells. Several methods have been developed to deal with electrical effects on the vicinity of a charged membrane. Numerical methods have been developed by the authors of the present paper [1,2] and, also, by other authors [3–7]. Karthik et al. [3], Sarkar et al. [4,5] and Sarkar and De [6,7] developed numerical codes to predict the permeate flux, the membrane surface concentration and the permeate concentration along the membrane length under a constant external electric field [3–7]. Karthik et al. [3] modelled and simulated the electric field enhanced cross flow ultrafiltration of a bovine serum albumin (BSA) solution under osmotic pressure-controlled regime.

*Corresponding author.

Sarkar et al. [4,5] studied the effect of the electric field during gel-layer-controlled ultrafiltration of synthetic juice and fruit juice [4] and predicted the permeate flux during osmotic pressure-controlled electric ultrafiltration [5]. Sarkar and De [6] developed a theoretical analysis based on an integral method for quantification of the permeate flux and mass transfer coefficient in gel-layer-controlled ultrafiltration enhanced by an electric field. They considered a developed mass transfer boundary layer under turbulent flow regime. Moreover, Sarkar and De [7] predicted the permeate flux for turbulent flow in a cross flow electric field assisted ultrafiltration. Apart from these studies applied to ultrafiltration processes, a constant external electric field is frequently used in electrodialysis processes. Electrodialysis is a separation process that arranges ion-exchange membranes alternately in a direct constant electric field [8]. This technique provides versatile tools for industrial separations and has received attention recently [8].

Pinto et al. developed a numerical code [1,2] to allow the determination of the flow, concentration and variable electric potential in a bidimensional membrane cell. The code allows the complete characterization of the transport of solutes in the vicinity of a charged membrane. Firstly, they studied the separation of ionic components assuming that the convective flow effect on the ionic distribution was negligible [1]. The electric potential was determined by a simplified method taking the Boltzmann distribution of the charged ions. In a second study [2], the complete Poisson–Boltzmann, Nernst–Planck and Navier–Stokes equations were solved simultaneously. A numerical method was developed to deal with the coupling between electric and concentration fields of all species in solution. The concentration, velocity and electric fields were obtained in a bidimensional domain. In these studies [1,2], the authors considered total rejection of the components by the membrane. However, in macromolecules fractionation, different components have different transmissions through the membrane pores [9–12], and so the code was improved to take them in consideration.

Most of the analytical methods in the literature are based on the stagnant film model. Following this model, an equation relating the permeate velocity with the electric field is derived from a mass balance to a stagnant film located in the vicinity of the membrane. Sarkar et al. [13] used the film model to establish the gel layer resistance in their study about fractionation of BSA and lysozyme (LYS) for several values of pH solution (7.4; 8.6; 11). The proteins have distinguished and opposite electric charges and the fractionation occurs under a constant external electric field. Rabiller-Baudry et al. [14] studied the application of a convective–diffusive–electrophoretic (CDE) migration model to the ultrafiltration of LYS. The CDE model developed accounts for the transfer of a charged solute (LYS) in the boundary layer of an ultrafiltration membrane. The authors assumed total rejection of LYS by the membrane. The study was done for different pH values of the solution and different ionic strengths of the solute. The model was used to determine the concentration of the solute at the membrane surface, as well as the solute concentration profiles in the polarized layer. Experimental data of the zeta-potential of the membrane, experimental electrophoretic mobility of the solute and convective and diffusive transport data of the solute were the inputs to the model. Rabiller-Baudry et al. [14] also compared the results obtained with the CDE model with data from a convective–diffusive model (CD). The concentration profiles along the boundary layer taken with the CDE model show a maximum in a very small distance to the membrane. This maximum is not predicted by the CD model [14]. Vasan et al. [15,16] also developed a model to determine the concentration profile of a charged solute in a polarized layer. The results showed an excellent agreement with the numerical/experimental data reported by Rabiller-Baudry et al. [14].

The stagnant film model is a crude approximation of the flow field in the vicinity of the membrane. The resulting film equation has, therefore, limitations. Miranda and Campos [17] studied the accuracy of the stagnant film model applied to a convective–diffusive transport (CD model), where the electrophoretic mobility of the solute was disregarded. The authors compared the Sherwood number of an impermeable cell (considering uniform mass production or uniform concentration at the wall), with the Sherwood number of a permeable cell predicted by the film equation using, as input, the surface concentrations and the permeate velocities obtained numerically through an in-house developed code. They concluded that the film equation (using Sherwood number of an impermeable cell) is accurate for low and moderate Peclet numbers and permeate velocities.

The accuracy of the stagnant film equation obtained from a CDE migration model is a topic not yet explored in the literature, as far as we know.

The present work contributes to the knowledge of the accuracy of the stagnant film equation applied to the study of electrophoretic migration of solutes near an ultrafiltration membrane. The film equation is a fast and easy tool to obtain permeate velocities in membrane separation processes.

A membrane separation process of two proteins with distinct electric charge and distinct molecular

weight (example: BSA and LYS) in an ionic solution of NaCl was considered to develop the present work. The separation occurs under electric interactions between membrane/components and through the transmission of the components acrossing the membrane.

The film equation was obtained from a mass balance in the neighbouring of an ultrafiltration membrane and it is supported on a CDE model. Two analytical models of CDE film equation were deducted: CDE I—non-linear electric potential and total rejection of the components by the membrane; CDE II—uniform electric field and transmission of the components through the membrane.

The accuracy of the film equation models was established through numerical computational fluid dynamics (CFD) results. The in-house code solves simultaneously all the conservative equations (Poisson–Boltzmann, Nernst–Planck and Navier–Stokes equations) and respective boundary conditions, considering transmission through the membrane. Permeate velocities, concentrations at membrane surface and rejection coefficients of the components, taken from the in-house numerical code, will be the input values to the film equation CDE. Sherwood number (Sh_i) obtained will be compared with the Sherwood number of an impermeable cell (Sh_i^I). The comparison will be done along the length of the membrane and for several values of non-dimensional numbers: $|z_i \times \Pi_3|$ (for film equation CDE ***I***) or $|z_i \times E|$ (for film equation CDE ***II***). Those ranges where the non-dimensional numbers Sh_i and Sh_i^I have identical values, will be the ranges where the permeate velocities can be accurately obtained using film equation CDE (***I*** or ***II***).

2. Cell description, general assumptions and physical properties

The parallel plate cell under study is composed by a membrane with negative zeta-potential, Φ_w, which is permeable to the solvent and partially permeable to the solutes (Fig. 1).

The feed stream is separated into two streams: the retentate stream, which leaves the cell through the principal channel and the permeate stream that crosses the membrane. The feed stream is composed by a mixture of two proteins, BSA and LYS, in an ionic solution of NaCl (Na^+ and Cl^-). The feed stream is electrically neutral.

The separation is done according to the solutes-membrane electric interactions and also to the transmission of the solutes through the membrane.

The characteristics of the cell are listed in Table 1. The cell is bidimensional—length (L_m) × height (H)—

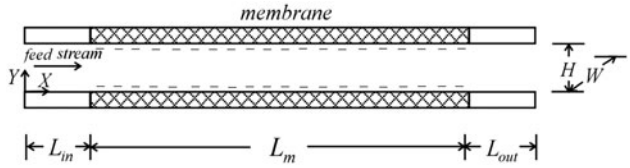

Fig. 1. Cell composed of a negatively charged membrane.

and so the width (W) is considered infinite. Moreover, the static pressure difference (ΔP_0) between the two sides of the membrane is 1×10^4 Pa.

Some general assumptions were considered:

- The pH of the buffer solution is constant and equal to 7.4;
- The osmotic pressures of the proteins, BSA and LYS, and of the ionic species, Na^+ and Cl^-, are considered negligible since the film equation is only valid under non-polarized conditions. Therefore, the concentrations of these species are, everywhere in the cell, including over the semi-permeable membranes, very low (dilute solution);
- The transport properties (viscosity and diffusivity) of all the species are considered constant. In a very diluted solution, viscosity and diffusivity are practically independent of the concentration of the species, including in the vicinity of the membrane surface;
- The viscosity of the solution is considered identical to that of pure water everywhere inside the cell (very diluted solution);
- Electric effects inside the membrane pores are not considered;
- The proteins are assumed to be non-interacting; diluted feed solution and low feed velocity were used to make this assumption accurate [10].

The properties of the proteins (BSA and LYS) and ions (Na^+ and Cl^-) of the solution are presented in Table 2.

The equivalent molecular radius (r_i^*) of proteins BSA and LYS are listed in Table 3. The equivalent molecular radius of BSA was determined from data

Table 1
Characteristics of the cell

Membrane	OMEGA polysulfone membrane 50 kDa MWCO
R_m	$5.714 \times 10^{12}\ m^{-1}$
H	0.001 m
L_m	0.040 m
$L_{in} = L_{out}$	0.02 m

Table 2
Properties of proteins, BSA and LYS, in an ionic solution of NaCl

Component	BSA[a]	LYS[a]	Na^{+}[a]	Cl^{-}[a]
M_i (kg/kmol)	69000	14600	23	35.45
Z_i	−21 [b]	+3 [c]	+1	−1
D_i (m^2/s)	7.0×10^{-11}[d]	11.8×10^{-11}[d]	1.33×10^{-9}[e]	2.30×10^{-9}[e]
C_i^o (kg/m^3)	6.90×10^{-5}	1.02×10^{-4}	2.30×10^{-8}	3.545×10^{-8}
C_{Mi}^o ($kmol/m^3$)	1.0×10^{-9}	7.0×10^{-9}	1.0×10^{-9}	1.0×10^{-9}

[a] solutes are those used by Sarkar et al. [13]; [b]electric charge of BSA was taken from Chun and Lee [18]; [c]electric charge of LYS was determined through its zeta-potential value - $\zeta_{LYS} = 6.7$ mV – Sarkar et al. [13]; [d]diffusivities of BSA and LYS were taken from Sarkar et al. [13]; [e]diffusivities of Na^+ and Cl^- were taken from Pivonka et al. [19].

Table 3
Values of equivalent molecular radius (r_i^*) for BSA and LYS

Component	r_i^* (nm)
BSA	3.04
LYS	2.09

of Tencer et al. [20] and the equivalent molecular radius of LYS from Sarkar et al. [13]. The specific area of the pores (s) of the OMEGA Polysulfone Membrane 50 kDa MWCO was obtained from experimental data of Opong and Zydney [11] and is equal to 1.86 nm.

Values of rejection coefficient (R_i) of the components were determined through a convective–diffusive transport model through the membrane developed by Opong and Zydney [11]. The transmission model was implemented in the numerical code. More details about the procedure are described in Pinto et al. [12].

3. Theory

3.1. Conservative equations and boundary conditions

The Poisson–Boltzmann (for the film equation CDE ***I***) or constant electric field (for the film equation CDE ***II***), the Nernst–Planck, the Navier–Stokes equations and respective boundary conditions were solved, simultaneously, by numerical methods CFD. Permeate velocities, surface concentrations and rejection coefficients of the components along the total length of the membrane, taken from the in-house code, are the input values to the film equation CDE ***I*** and ***II***.

The equations were solved in the numerical domain represented in Fig. 2. Grid for simulations was selected after performing several grid tests according to the procedure described by Pinto et al. [1,2]. The grid selected is composed by 117×501 nodes.

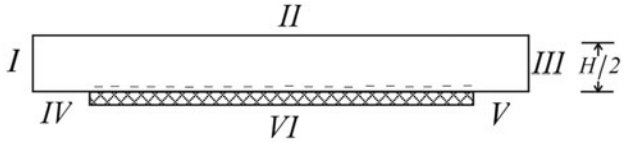

Fig. 2. Schematic representation of the domain of a cell with a permeable membrane and respective boundaries (I – cell inlet; II – symmetric axis; III – cell outlet; IV – impermeable wall; V – impermeable wall; VI – membrane with negative zeta-potential).

In the conservative equations described below, the uppercase variables symbolize dimensional variables and the lowercase normalized variables. The electric potential is normalized by the absolute value of the membrane potential (Φ_w), concentrations by the inlet concentrations of the solutes (C_i^0), velocities by the inlet velocity (V_0) and geometric dimensions by the height of the cell (H).

The conservative electric potential equation, Poisson–Boltzmann equation, used to study the accuracy of film equation CDE ***I***, is:

$$\frac{\partial \phi}{\partial t} = \left(\frac{\partial^2 \phi}{\partial x^2} + \frac{\partial^2 \phi}{\partial y^2}\right) + \Pi_2 r_e \tag{1}$$

where ϕ is the non-dimensional electric potential, r_e the sum of the ionic concentrations of all the components and Π_2 a non-dimensional electric number defined by:

$$\Pi_2 = \frac{F C_{ref}^0 H^2}{\varepsilon M_{ref} \Phi_w} \tag{2}$$

where F is the Faraday constant, C_{ref}^0 the concentration of the reference component in the bulk, M_{ref} the molar mass of the reference component and ε the permittivity. The cation, Na^+, was arbitrarily chosen as the reference component.

The sum of the normalized ionic concentrations was determined according to the local ionic concentrations:

$$r_e = \sum_{t=1}^{N} z_i \frac{C_i^0}{C_{ref}^0} \frac{M_{ref}}{M_i} c_i \tag{3}$$

where z_i is the electric charge of component i, c_i the normalized concentration of component i and M_i the molar mass of component i. The index *ref* refers to the reference component.

A constant electric field (E_f) was considered to study the accuracy of film equation CDE ***II***. The constant electric field is defined by:

$$\frac{\partial \Phi}{\partial Y} = -E_f \tag{4}$$

or after normalization by:

$$\frac{\partial \phi}{\partial y} = -E \tag{5}$$

where the non-dimensional number E is given by:

$$E = \frac{E_f H}{\Phi_w} \tag{6}$$

Then, the linear electric potential equation becomes:

$$\phi = \phi_w - Ey \tag{7}$$

where ϕ_w is the normalized electric potential at the membrane surface.

The Navier–Stokes, Nernst–Planck equations and boundary conditions are described in Appendix A. The convergence of the numerical method is also shown in Appendix B.

3.2. Film equation

A mass balance considering convection, diffusion, electrophoretic mobility and transmission through the membrane, to a stagnant film in the vicinity of the membrane surface is schematically represented in Fig. 3.

The equation representing the mass balance is:

$$V_m C_i = -D_i \frac{dC_i}{dY} - \mu_i C_i \frac{d\Phi}{dY} + \mu_i C_i^P \left.\frac{d\Phi}{dY}\right|_{Y=0} + V_m C_i^p \tag{8}$$

where V_m is the velocity at the membrane surface, D_i the diffusivity of component i, C_i the concentration of component i, C_i^p the concentration of component i in the permeate flux, Φ the electric potential and μ_i the electrophoretic mobility of component i. The electrophoretic mobility is given by:

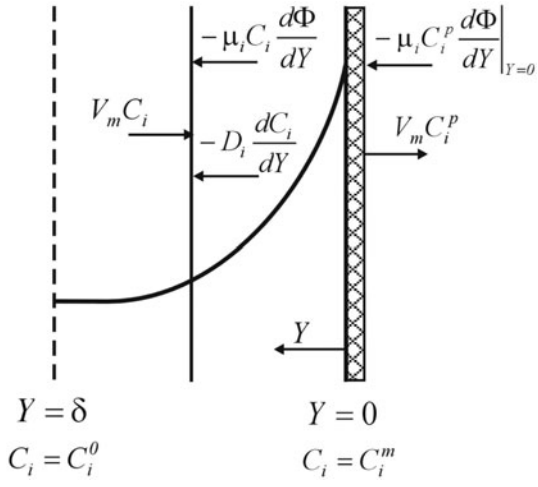

Fig. 3. Mass balance to the control volume in the boundary layer at the membrane surface.

$$\mu_i = z_i \frac{FD_i}{RT} \tag{9}$$

where z_i is the electric charge of component i.

The mass boundary conditions (Fig. 3) are:

$$\begin{cases} C_i = C_i^0 \rightarrow Y = \delta \\ C_i = C_i^m \rightarrow Y = 0 \end{cases} \tag{10}$$

where C_i^0 is the concentration of component i in the feed solution, C_i^m the concentration of component i at the membrane surface and δ the thickness of the boundary layer.

According to the Debye approximation (for $\Phi < 27$ mV) [14], the electric potential (Φ) changes in a non-linear way along the normal direction Y to the membrane:

$$\Phi = \Phi_w e^{-k_{Db} Y} \tag{11}$$

where k_{Db} is the reciprocal of the Debye length, which at 25°C is given by:

$$k_{Db} = 3.28 \times 10^9 \times I^{0.5} \tag{12}$$

where I is the ionic strength in mol L^{-1}.

Taking non-dimensional variables, the mass balance equation becomes:

$$\frac{dc_i}{dy} = -\mathrm{Pe}_i v_m (c_i - c_i^p) + z_i \Pi_3 k_{Db} H (c_i e^{-k_{Db} y H} - c_i^P) \tag{13}$$

According to the equation, the concentration profile depends on the Peclet number of component i (Pe_i) and on the non-dimensional electric number Π_3.

However, Eq. (13) can only be solved by numerical methods (e.g. Euler´s method [21]).

Two versions of the film equation CDE were developed assuming simplifications: one for total rejection of the components through the membrane and a non-linear electric potential along the normal direction to the membrane—film equation CDE ***I***; another considers transmission of the components through the membrane and a linear electric potential along the normal direction to the membrane—film equation CDE ***II***.

3.2.1. Total rejection and non-linear electric potential (I)

Supposing total rejection, $C_i^p = 0$, the mass balance becomes:

$$V_m C_i = -D_i \frac{dC_i}{dY} - \mu_i C_i \frac{d\Phi}{dY} \tag{14}$$

The Debye approximation (for $\Phi < 27\,\text{mV}$ [14]), Eq. (11), is taken to represent the non-linear relation between the electric potential (Φ) and the normal direction Y to the membrane.

Then, integrating Eq. (14) with mass boundary conditions (10), the film equation CDE ***I***, is:

$$V_m = \frac{D_i}{\delta}\left[\ln\left(\frac{C_i^m}{C_i^0}\right) + z_i \Pi_3 [1 - \exp(-k_{Db}\delta)]\right] \tag{15}$$

and taking non-dimensional variables becomes:

$$v_m = \frac{\text{Sh}_i}{\text{Pe}_i}\left[\ln(c_i^m) + z_i \Pi_3 \left[1 - \exp\left(-\frac{k_{Db}H}{\text{Sh}_i}\right)\right]\right] \tag{16}$$

According to the equation, the normalized permeate velocity (v_m) depends on the normalized concentration of component i at the membrane surface (c_i^m) and on the Sherwood number of component i (Sh_i) defined by:

$$\text{Sh}_i = \frac{k_i H}{D_i} \tag{17}$$

where k_i is the mass transfer coefficient of component i given by:

$$k_i = \frac{D_i}{\delta} \tag{18}$$

Previous work [17] has shown that the appropriate Sherwood number for the film equation is the Sherwood number of the analogous impermeable cell (Sh_i^I):

$$v_m = \frac{\text{Sh}_i^I}{\text{Pe}_i}\left[\ln(c_i^m) + z_i \Pi_3 \left[1 - \exp\left(-\frac{k_{Db}H}{\text{Sh}_i^I}\right)\right]\right] \tag{19}$$

3.2.2. Transmission of the components and constant electric field (II)

The other film equation (***II***) based on a CDE model is established considering a constant electric field (E_f) defined by Eq. (4). An analytical equation can be obtained even for transmission of the components through the membrane ($C_i^p \neq 0$).

The mass balance near the membrane surface becomes:

$$V_m C_i = -D_i \frac{dC_i}{dY} - \mu_i(-E_f)(C_i - C_i^p) + V_m C_i^p \tag{20}$$

Then, replacing C_i^p by $C_i^m(1 - R_i)$ and integrating Eq. (20) with mass boundary conditions (10), the film equation CDE ***II***, is expressed by:

$$V_m - \mu_i E_f = \frac{D_i}{\delta}\left[\ln\left(\frac{R_i C_i^m}{C_i^0 - (1 - R_i)C_i^m}\right)\right] \tag{21}$$

After normalization the film equation becomes:

$$v_m - \frac{\mu_i E_f}{V_0} = \frac{\text{Sh}_i^I}{\text{Pe}_i}\left[\ln\left(\frac{R_i c_i^m}{1 - (1 - R_i)c_i^m}\right)\right] \tag{22}$$

3.2.3. Evaluation of the accuracy of the film equation

The accuracy of the film equation can be evaluated by comparing the Sherwood number for an impermeable system, Sh_i^I, with the Sherwood number given by the film equation, Sh_i^{In}. In the case of the film equation CDE ***I***, the following equation, to determine Sh_i^{In}, is used:

$$\text{Sh}_i^{In} = \frac{v_m \text{Pe}_i}{\ln(c_i^m) + z_i \Pi_3 \left[1 - \exp\left(-\frac{k_{Db}H}{\text{Sh}_i^{\text{In}}}\right)\right]} \tag{23}$$

If electric interactions are negligible, Eq. (23) becomes:

$$\text{Sh}_i^{In} = \frac{v_m \text{Pe}_i}{\ln(c_i^m)} \tag{24}$$

In the case of film equation CDE ***II***, the Sherwood number given by the film equation is:

$$\mathrm{Sh}_i^{ln} = \frac{\left(v_m - \frac{\mu_i E_f}{V_0}\right)\mathrm{Pe}_i}{\ln\left(\frac{R_i c_i^m}{1-(1-R_i)c_i^m}\right)} \quad (25)$$

If electric effects are negligible, Eq. (25) becomes:

$$\mathrm{Sh}_i^{ln} = \frac{v_m \mathrm{Pe}_i}{\ln\left(\frac{R_i c_i^m}{1-(1-R_i)c_i^m}\right)} \quad (26)$$

The values of c_i^m, v_m and R_i will be determined by the numerical code. For film equation CDE ***I***, c_i^m and v_m were taken considering Poisson–Boltzmann equation and total rejection coefficient. For film equation CDE ***II***, they were taken assuming constant electric field and transmission of the components through the membrane.

4. Results and discussion

The Sherwood numbers of the components along the length of the membrane x, predicted by Eqs. (23) and (25), are compared with the Sherwood numbers in an impermeable cell. This comparison is done to study the range of applicability of the film equation. The effect of the electrical interactions on the applicability of the film equation is determined by studying the effect of the non-dimensional numbers $|z_i \times \Pi_3|$ (for film equation CDE ***I***) and $|z_i \times E|$ (for film equation CDE ***II***).

Reynolds number of the solution and Peclet number of each component are represented in Table 4.

4.1. Range of applicability of the film equation CDEI (*non-linear electric potential*)

Sherwood number profiles of BSA and LYS are in Fig. 4(a) and (b). Three Sherwood number profiles are represented: the Sherwood profile determined by the film equation based in a CD model—Eq. (24), the Sherwood profile determined by the film equation (***I***) based on a CDE model—Eq. (23), and the Sherwood profile for an impermeable cell. While the Sherwood number profiles based on the CDE model are coincident with the Sherwood profile for an impermeable cell, the Sherwood profiles obtained with the CD model are higher (BSA) and lower (LYS). This behavior stresses the importance of the electric effects to make predictions with the film equation.

Table 4
Reynolds number (Re) of the solution and Peclet number of each component ($\mathrm{Pe_{BSA}}$, $\mathrm{Pe_{LYS}}$, $\mathrm{Pe_{Na+}}$, $\mathrm{Pe_{cl}^-}$)

Re	95
$\mathrm{Pe_{BSA}}$	1.36×10^6
$\mathrm{Pe_{LYS}}$	8.05×10^5
$\mathrm{Pe_{Na+}}$	7.14×10^4
$\mathrm{Pe_{Cl}^-}$	4.68×10^4

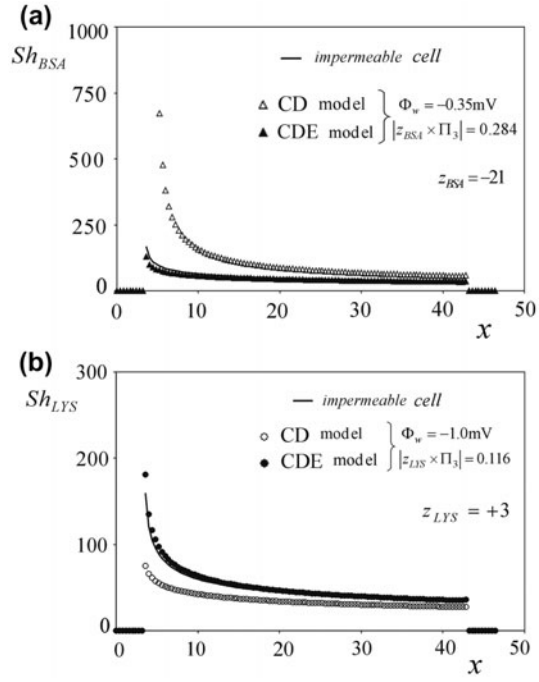

Fig. 4. Sherwood number along the length of the membrane, x, determined through film equations (CD and CDE model – film equation ***I***): (a) BSA; (b) LYS.

The accuracy of the film equation CDE ***I*** depends on the non-dimensional number $|z_{\mathrm{BSA}} \times \Pi_3|$. Fig. 5 shows the Sherwood number profiles of BSA and LYS, determined by Eq. (23). Total rejection of both components was considered in the numerical calculations. Fig. 5(a) and (b) show Sherwood profiles for low zeta-potential values of a negatively charged membrane while Fig. 5 (c) and (d) represent the Sherwood profiles for high zeta-potential values of a negatively charged membrane. When the non-dimensional number $|z_{\mathrm{BSA}} \times \Pi_3|$ is lower than 0.284 (Fig. 5a), the Sherwood profiles of BSA are independent of the electric potential at the membrane surface and they are equal to the Sherwood profile in an impermeable cell. When the non-dimensional number $|z_{\mathrm{BSA}} \times \Pi_3|$ is high, for example, $|z_{\mathrm{BSA}} \times \Pi_3| = 8.119$ (Fig. 5c), the membrane, with a strong negative zeta-potential ($\Phi_w = -10$ mV) combined with the high negative BSA charge ($z_{\mathrm{BSA}} = -21$), induces a strong BSA repulsion by the membrane. A maximum

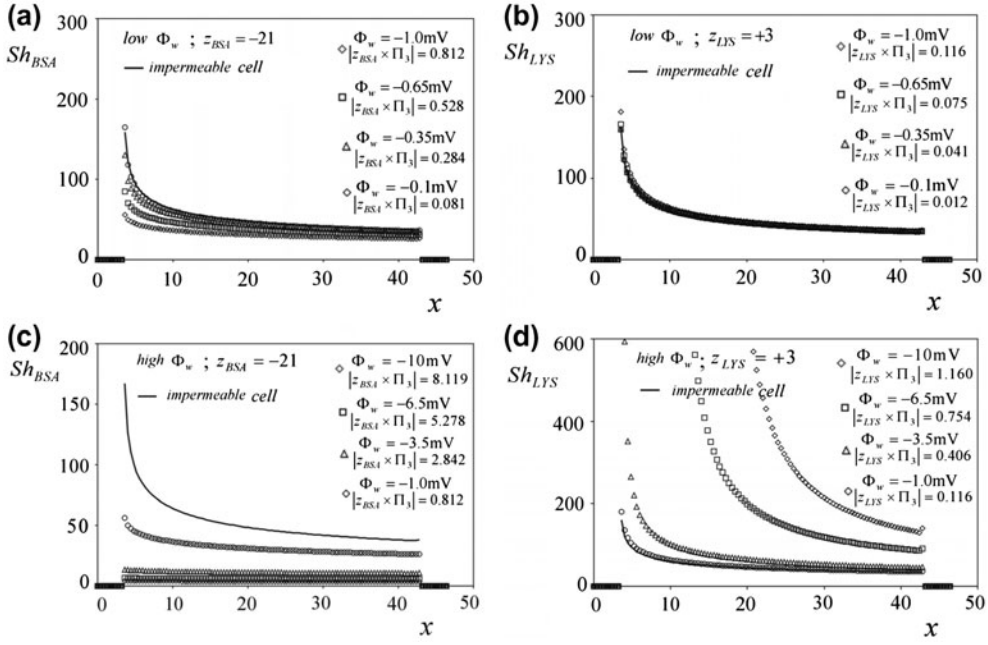

Fig. 5. Sherwood number along the length of the membrane, x, determined thought film equation CDE ***I***: (a) for BSA and low zeta-potential values at the membrane surface; (b) for LYS and low zeta-potential values at the membrane surface; (c) for BSA and high zeta-potential values at the membrane surface; (d) for LYS and high zeta-potential values at the membrane surface.

of BSA concentration (Fig. 6), at the end of the membrane and far from the surface, can be observed, see Fig. 6. At the membrane surface, the normalized BSA concentrations are lower than 1, that is, the concentrations at the membrane surface are lower than the concentrations in the bulk (Fig. 6).

For a non-dimensional number $|z_{\mathrm{LYS}} \times \Pi_3|$ lower than 0.116 (see Fig. 5(b) and (d)), Sherwood profiles of LYS overlap and are equal to the Sherwood profile in an impermeable cell. When the potential at the membrane surface is higher (e.g. $|z_{\mathrm{LYS}} \times \Pi_3| = 1.160$), Sherwood number is much higher than that in an impermeable cell (Fig. 5d). For $|z_{\mathrm{LYS}} \times \Pi_3| = 1.160$, LYS (electric charge equal to +3) is strongly attracted to the membrane and its concentration increases with higher percentage (Fig. 7) comparatively to the concentration when $|z_{\mathrm{LYS}} \times \Pi_3| = 0.116$. Film equation ***I*** based on the CDE model is accurate, that is, Sherwood number of an impermeable cell can be used in the film equation, for a component i, when the value of the non-dimensional number $|z_i \times \Pi_3|$ is lower than 0.284.

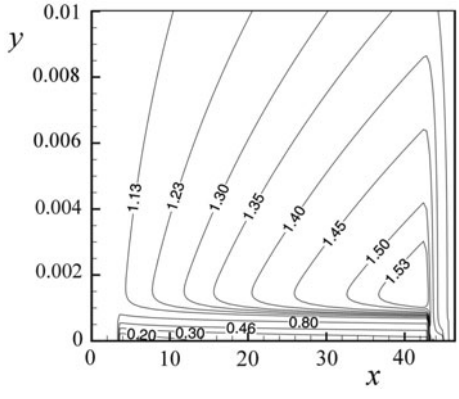

Fig. 6. BSA iso-concentration lines for $\Phi_w = -10$ mV $= (|z_{\mathrm{BSA}} \times \Pi_3| = 8.119)$, $\Pi_1 = 1.07 \times 10^{-4}$, $\Pi_2 = 1.36 \times 10^5$, $\Pi_3 = 0.387$.

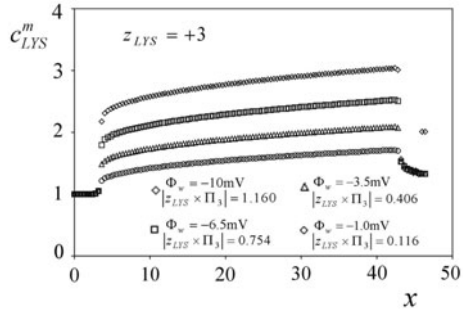

Fig. 7. LYS normalized concentration profiles along the longitudinal direction x and for different values of zeta-potential at the membrane surface: ($\Phi_w = -10mV$ ($|z_{\mathrm{LYS}} \times \Pi_3| = 1.160$), $\Phi_w = -6.5mV$($|z_{LYS} \times \Pi_3| = 0.754$), $\Phi_w = -3.5mV$ ($|z_{LYS} \times \Pi_3| = 0.406$), $\Phi_w = -1.0mV$($|z_{LYS} \times \Pi_3| = 0.116$).

4.2. Range of applicability of the film equation CDE II (constant electric field)

Fig. 8 shows Sherwood profiles of BSA and LYS along the surface of the membrane. Three Sherwood number profiles are represented: the Sherwood profile determined by the film equation based on the CD model, Eq. (26), the Sherwood profile determined by the film equation (***II***) based on the CDE model, Eq. (25), and the Sherwood profile for an impermeable cell. The Sherwood profiles determined by the film equation (***II***) based on the CDE model are coincident with the Sherwood profile for an impermeable cell. Those based on the CD model over-predict (BSA) and under-predict (LYS) the Sherwood profile for an impermeable cell. This behavior illustrates, once again, the importance of the electric term of the film equation.

Film equation CDE ***II*** was used to determine the Sherwood profiles along the membrane for several values of constant electric field (E_f). For non-dimensional number $|z_{\mathrm{BSA}} \times E|$ of BSA lower than 21 (Fig. 9(a)) and for non-dimensional number $|z_{\mathrm{LYS}} \times E|$ of LYS lower than 60 (Fig. 9(b)), Sherwood number profiles are coincident along the longitudinal direction x of the membrane. The Sherwood profiles are also identical to those in an impermeable cell (Fig. 9(a) and (b)) along the total length of the membrane.

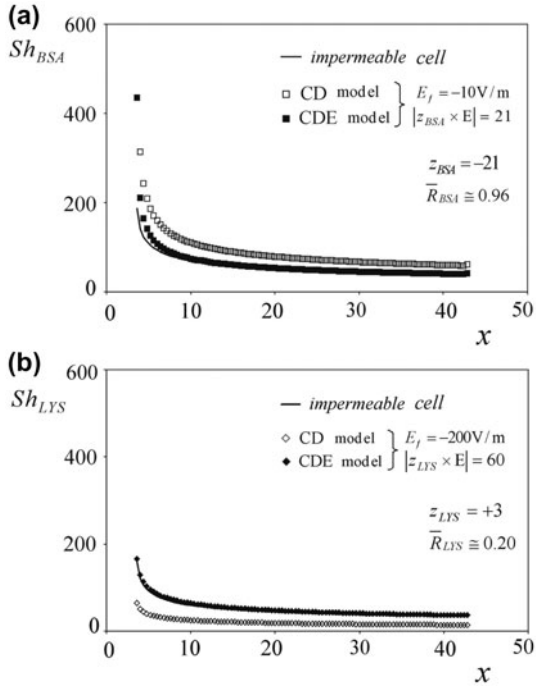

Fig. 8. Sherwood number along the length of the membrane, x, determined through film equations (CD and CDE model – film equation ***II***) (a) BSA; (b) LYS.

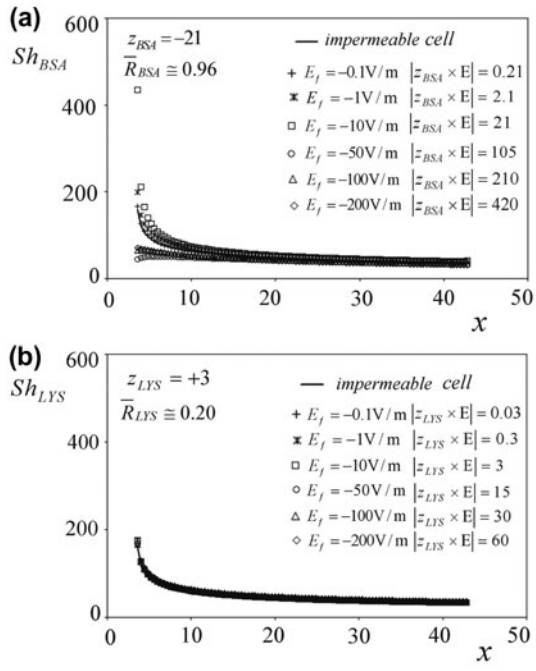

Fig. 9. Sherwood number profiles along the length of the membrane, x, determined thought film equation CDE ***II*** for: (a) BSA; (b) LYS; and different values of constant electric field: $E_f = -0.1$ V/m, $E_f = -1$ V/m, $E_f = -10$ V/m, $E_f = -50$ V/m, $E_f = -100$ V/m, $E_f = -200$ V/m.

However, for values of non-dimensional number $|z_{\mathrm{BSA}} \times E|$ of BSA higher than 105, there is a non-overlapping of BSA Sherwood number profiles (Fig. 9(a)) at the beginning of the membrane ($x < 15$). The inaccuracy of the film equation for $|z_{\mathrm{BSA}} \times E| \geqslant 105$ is associated with very low BSA concentrations at the membrane surface (Fig. 10). Since the repulsion of BSA from the membrane surface is high, the concentration over the membrane surface becomes much lower than the concentration in the bulk (normalized

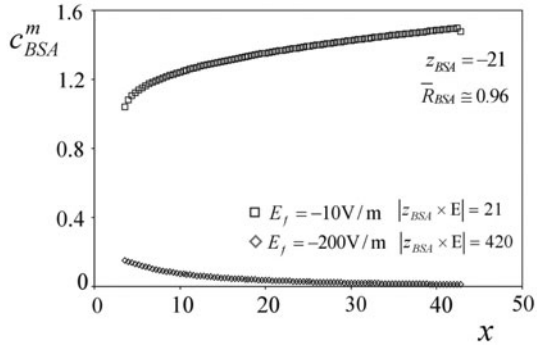

Fig. 10. BSA normalized concentration profiles along the longitudinal direction, x, of the membrane, for two values of constant electric field: $E_f = -10$ V/m($|z_{BSA} \times E| = 21$); $E_f = -200$ V/m ($|z_{BSA} \times E| = 420$).

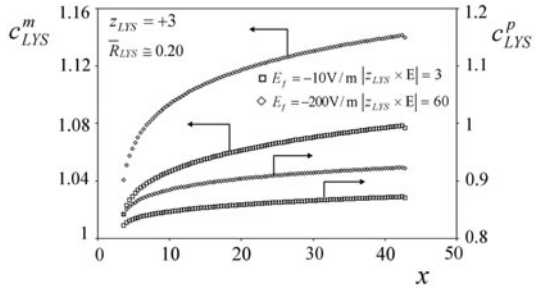

Fig. 11. LYS normalized concentration profiles at the membrane surface and in the permeate stream along the tangential direction, x, for two values of constant electric field: $E_f = -10$ V/m ($|z_{LYS} \times E| = 3$) and $E_f = -200$ V/m ($|z_{LYS} \times E| = 60$).

concentration lower than 1—Fig. 10) and it decreases along the membrane surface (Fig. 10).

For values of $|z_{\mathrm{LYS}} \times E| \leqslant 60$ (Fig. 9b), the LYS concentration at the membrane surface increases moderately along the length of the membrane (Fig. 11). Since LYS has an electric charge +3, its attraction to the negatively charged membrane surface is not so strong compared with the repulsion of BSA. Moreover, LYS is also the component with higher transmission through the membrane. For these reasons, LYS Sherwood profile determined by film equation CDE ***II*** is coincident, along the total length of the membrane, with Sherwood profile of an impermeable cell.

Film equation ***II*** based on CDE model is accurate, that is, Sh_i^I can be used in the film equation when the value of non-dimensional number $|z_i \times E|$ of component i is lower than 60.

5. Conclusions

Two versions of the film equation based on a CDE model were developed: one supposing total rejection of the components and a non-linear variation of the electric potential along the normal direction Y to the membrane—film equation ***I***; other considering transmission of the components through the membrane pores and a constant electric field—film equation ***II***.

The applicability of the film equations CDE was studied. Sherwood number profiles of BSA and LYS, along the length of the membrane, obtained with the film equations CDE (***I*** and ***II***) were compared with the Sherwood number profile of an impermeable cell. Normalized concentrations, normalized permeate velocities and rejection coefficients along the length of the membrane, obtained through a numerical code developed to solve the conservative equations, were used as input into the film equations.

For the film equation CDE ***I***, the Sherwood number obtained by the film equation is independent of the electric potential at the membrane surface (Φ_w) for values of the non-dimensional number $|z_i \times \Pi_3|$ lower than 0.284. Considering constant electric field, film equation CDE ***II***, Sherwood number profile is also independent of the constant electric field (E) along the membrane, for values of the non-dimensional number $|z_i \times E|$ lower than 60. For both ranges of the non-dimensional numbers, $|z_i \times \Pi_3|$ and $|z_i \times E|$, Sherwood number profiles are also equal to that in an impermeable cell. The film equations, with Sh_i^I, are then accurate for these ranges.

Notation

C_i — concentration of component i
c_i — normalized concentration of component i
$c^k_{g,h}$ — normalized concentration of a component in a node (g,h) at a current iteration k
C^0_i — concentration of component i at the feed/bulk
C^0_{ref} — concentration of the reference component at the feed/bulk
$C^0_{M,i}$ — molar concentration of component i at the feed/bulk
C^m_i — concentration of component i at membrane surface
c^m_i — normalized concentration of component i at membrane surface
C^p_i — concentration of component i in the permeate flux
c^p_i — normalized concentration of component i in the permeate flux
$c^k_{i,crit}$ — normalized concentration of component i on a critical location
D_i — molecular diffusivity of component i
$D_{i,eff}$ — effective diffusivity of component i along the membrane pores
E_f — constant electric field
F — Faraday constant
H — distance between parallel plates
I — ionic strength
k — current time step
k_i — mass transfer coefficient of component i
k_{Db} — reciprocal of the Debye length
L_{out} — length of the outlet section
L_{in} — length of the inlet section
L_m — total length of the membrane
L — total length of the cell
M_i — molar mass of component i
M_{ref} — molar mass of the reference component
R — gas constant
R_i — local rejection coefficient of component i

$\overline{R}_i$ — mean rejection coefficient of component i along the total length of the cell
$R_{g,1}$ — rejection coefficient of a component in a node $(g,1)$ at membrane surface
R_m — membrane resistance of the semi-permeable membrane
R_ϕ — sum of the residues of the electric potential equation
r_e — sum of the normalized ionic concentrations
r_i^* — equivalent molecular radius of component i
S_i — real transmission of component i
$S_{i,\infty}$ — asymptotic intrinsic sieving coefficient of component i
s — specific area of the pores of the membrane
T — temperature
t — non-dimensional time
V_0 — mean feed velocity
V_x — longitudinal component of the velocity
v_x — normalized longitudinal component of the velocity
$\hat{v}_{xi}$ — normalized pseudo-velocity in the longitudinal direction, x, of component i
V_y — vertical component of the velocity
v_y — normalized vertical component of the velocity
V_m — velocity at membrane surface (vertical component)
v_m — normalized velocity at membrane surface (vertical component)
$\hat{v}_{yi}$ — normalized pseudo-velocity in vertical direction, y, of component i
$\hat{v}_{y_{g,h}}$ — normalized pseudo-velocity (component y) in a node (g,h)
$\hat{v}_{y_{g,1}}$ — normalized pseudo-velocity (component y) in a node $(g,1)$
$\hat{v}_{yu}^m$ — incoming pseudo-velocity (normal direction) to the discretized node $(g,1)$ at membrane surface
$\hat{v}_{yd}^m$ — outgoing pseudo-velocity (normal direction) from the discretized node $(g,1)$ at membrane surface
W — width of the cell
X — longitudinal coordinate
x — normalized longitudinal coordinate
Y — vertical coordinate
y — normalized vertical coordinate
z_i — electric charge of component i

Non-dimensional numbers

Pe_i — Peclet number of component i: $\mathrm{Pe}_i = \frac{V_0 H}{D_i}$
Re — Reynolds number of the solution: $\mathrm{Re} = \frac{\rho V_0 H}{\overline{\mu}}$
Sh_i — Sherwood number of component i
Sh_i^I — Sherwood number of component i in an impermeable cell
Sh_i^{In} — Sherwood number of component i given by film equation
E — non-dimensional number defined by equation 8
Π_1 — non-dimensional electric number: $\Pi_1 = \frac{FC_{ref}^0 \Phi_w}{M_{ref} \rho V_0^2}$
Π_2 — non-dimensional electric number: $\Pi_2 = \frac{FC_{ref}^0 H^2}{\varepsilon M_{ref} \Phi_w}$
Π_3 — non-dimensional electric number: $\Pi_3 = \frac{F\Phi_w}{RT}$

Greek symbols

ΔP_0 — static pressure difference across the semi-permeable membrane
Δt — time step range
Δy — step range in the normal direction
ε — permittivity
$\varepsilon_{ci_{crit}}$ — numerical error of the concentration of component i in a critical location
$\varepsilon_{\phi_{crit}}$ — numerical error of the electric potential in a critical location
$\varepsilon_{\omega_{crit}}$ — numerical error of the vorticity in a critical location
ψ — stream function
ω — vorticity
ω_{crit}^k — vorticity in a critical location
ρ — density
μ_i — electrophoretic mobility of component i
$\overline{\mu}$ — mean viscosity of the solution
$\overline{\mu}_p$ — mean viscosity at the permeate flux
δ_m — membrane thickness
δ — thickness of the boundary layer
σ_{ap} — apparent selectivity
Φ — electric potential
ϕ — normalized electric potential
Φ_w — membrane electric potential
ϕ_w — normalized membrane electric potential
ϕ_{crit}^k — normalized electric potential in a critical location
ζ_i — zeta-potential of component i

Acknowledgements

The authors gratefully acknowledge the financial support of Fundação para a Ciência e Tecnologia (FCT) through project POCI/EQU/59724/2004 and scholarship SFRH/BD/27821/2006. POCTI (FEDER) also supported this work via CEFT.

References

[1] S.I.S. Pinto, J.M. Miranda, J.B.L.M. Campos, Numerical study of the effect of a charged membrane in the separation of electrically charged components, Desalin. Water Treat. 14 (2010) 201–207.
[2] S.I.S. Pinto, J.M. Miranda, J.B.L.M. Campos, Interaction between the electric and concentration fields in the fractionation of two macromolecules using a hybrid membrane cell—CFD study, Desali. Water Treat. 35 (2011) 209–221.
[3] V. Karthik, S. DasGupta, S. De, Modeling and simulation of osmotic pressure controlled electro-ultrafiltration in a cross-flow system, J. Membr. Sci. 199 (2002) 29–40.

[4] B. Sarkar, S. DasGupta, S. De, Effect of electric field during gel-layer controlled ultrafiltration of synthetic and fruit juice, J. Membr. Sci. 307 (2008) 268–276.
[5] B. Sarkar, S. DasGupta, S. De, Prediction of permeate flux during osmotic pressure-controlled electric field-enhanced cross-flow ultrafiltration, J. Colloid Interf. Sci. 319 (2008) 236–246.
[6] B. Sarkar, S. De, Electric field enhanced gel controlled cross-flow ultrafiltration under turbulent flow conditions, Sep. Purif. Technol. 74 (2010) 73–82.
[7] B. Sarkar, S. De, Prediction of permeate flux for turbulent flow in cross-flow electric field assisted ultrafiltration, J. Membr. Sci. 369 (2011) 77–87.
[8] T. Xu, C. Huang, Electrodialysis—based separation technologies: a critical review, AIChE J. 54 (2008) 3147–3159.
[9] W.M. Deen, Hindered transport of large molecules in liquid-filled pores, AIChE J. 33 (1987) 1409–1425.
[10] R. Ghosh, Z.F. Cui, Simulation study of the fractionation of proteins using ultrafiltration, J. Membr. Sci. 180 (2000) 29–36.
[11] W.S. Opong, A.L. Zydney, Diffusive and convective protein transport through asymmetric membranes, AIChE J. 37 (1991) 1497–1510.
[12] S.I.S. Pinto, J.M. Miranda, J.B.L.M. Campos, Use of hybrid membrane cells to improve the apparent selectivity in the fractionation of two components—CFD study, Ind. Eng. Chem. Res. 49 (2010) 9978–9987.
[13] B. Sarkar, S. DasGupta, S. De, Electric field enhanced fractionation of protein mixture using ultrafiltration, J. Membr. Sci. 341 (2009) 11–20.
[14] M. Rabiller-Baudry, B. Chaufer, P. Aimar, B. Bariou, D. Lucas, Application of a convection–diffusion–electrophretic migration model to ultrafiltration of lysozyme at different pH values and ionic strengths, J. Membr. Sci. 179 (2000) 163–174.
[15] S.S. Vasan, R.W. Field, Z. Cui, A Maxwell–Stefan–Gouy–Debye model of the concentration profile of a charged solute in the polarization layer, Desalination 192 (2006) 356–363.
[16] S.S. Vasan, C.D. Bain, R.W. Field, Z. Cui, A Maxwell–Stefan–Derjaguin–Graham model of the concentration profile of a charged solute in the polarization layer, Desalination 200 (2006) 175–177.
[17] J.M. Miranda, J.B.L.M. Campos, Mass transfer in the vicinity of a separation membrane—the applicability of the stagnant fluid theory, J. Membr. Sci. 202 (2002) 137–150.
[18] M.-S. Chun, I. Lee, Rigorous estimation of effective protein charge from experimental electrophoretic mobilities for proteomics analysis using microchip electrophoresis, Colloids Surf. A 318 (2008) 191–198.
[19] P. Pivonka, C. Hellmich, D. Smith, Microscopic effects on chloride diffusivity of cement pastes—a scale transition analysis, Cem. Concr. Res. 34 (2004) 2251–2260.
[20] M. Tencer, R. Charbonneau, N. Lakoud, P. Berini, AFM study of BSA adlayers on Au stripes, Appl. Surf. Sci. 253 (2007) 9209–9214.
[21] S. Chapra, R. Canale, Numerical Methods for Engineers with Software and Programming Applications, fourth ed., McGraw-Hill – International Edition, New York, USA, 2002.
[22] S.I.S. Pinto, T.M.G.T. Rocha, J.M. Miranda, J.B.L.M. Campos, A new membrane fractionation process based on the combination of hybrid membrane cells and differential diffusion of two solutes, Desalination 241 (2009) 372–387.
[23] H. Lonsdale, U. Merten, R. Riley, Transport properties of cellulose acetate osmotic membranes, J. Appl. Polym. Sci. 9 (1965) 1341–1358.
[24] S.I.S. Pinto, J.M. Miranda, J.B.L.M. Campos, A numerical study of the apparent selectivity in the fractionation of two macromolecules by ultrafiltration, Sep. Sci. Technol. 47 (2012) 936–949.

Appendix A

Navier–Stokes, Nernst–Planck equations and boundary conditions

The flow in the cell is described by the Navier–Stokes equations. In cartesian coordinates (x and y), the vorticity transport equation is given by:

$$\frac{\partial \omega}{\partial t} + v_x \frac{\partial \omega}{\partial x} + v_y \frac{\partial \omega}{\partial y} = \frac{1}{\mathrm{Re}} \left(\frac{\partial^2 \omega}{\partial x^2} + \frac{\partial^2 \omega}{\partial y^2} \right) - \Pi_1 \left(\frac{\partial r_e}{\partial y} \frac{\partial \phi}{\partial x} - \frac{\partial r_e}{\partial x} \frac{\partial \phi}{\partial y} \right) \quad (A.1)$$

Re is the Reynolds number and Π_1 a non-dimensional electric number defined by:

$$\Pi_1 = \frac{F C^0_{ref} \Phi_w}{M_{ref} \rho V_0^2} \quad (A.2)$$

where ρ is the fluid density and V_0 the feed velocity.

The Poisson equation for the stream function is:

$$\omega = \frac{\partial^2 \psi}{\partial x^2} + \frac{\partial^2 \psi}{\partial y^2} \quad (A.3)$$

and the velocity components are related to the stream function by:

$$v_x = \frac{\partial \psi}{\partial y}; \quad v_y = -\frac{\partial \psi}{\partial x} \quad (A.4)$$

The Nernst–Planck equation of each component i is given by:

$$\frac{\partial c_i}{\partial t} + \frac{\partial (\hat{v}_{xi} c_i)}{\partial x} + \frac{\partial (\hat{v}_{yi} c_i)}{\partial y} = \frac{1}{\mathrm{Pe}_i} \left(\frac{\partial c_i^2}{\partial x^2} + \frac{\partial c_i^2}{\partial y^2} \right) \quad (A.5)$$

where

$$\hat{v}_{xi} = \left(v_x - \frac{z_i \Pi_3}{\mathrm{Pe}_i} \frac{\partial \phi}{\partial x} \right) \quad (A.6)$$

$$\hat{v}_{yi} = \left(v_y - \frac{z_i \Pi_3}{\mathrm{Pe}_i} \frac{\partial \phi}{\partial y} \right) \quad (A.7)$$

The pseudo-velocity components, $\hat{v}_{xi}$ and $\hat{v}_{yi}$, are specific of each component i, since they depend on the respective Peclet number (Pe_i) and on the non-dimensional electric number Π_3 defined by.

$$\Pi_3 = \frac{F \Phi_w}{RT} \quad (A.8)$$

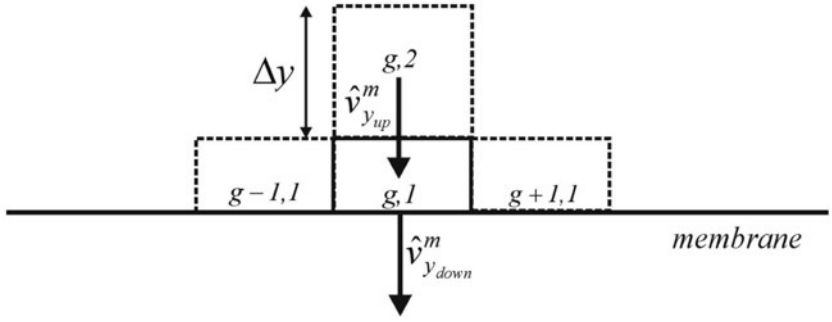

Fig. 1A. Discretization detail at the membrane surface.

More details about the discretization and iterative method are described by Pinto et al. [1,2]. Conditions for boundaries I–V (Fig. 2) are also given by Pinto et al. [1,2,22]. However, in those studies [1,2,22], the membrane totally rejects the solutes and so the numerical code used in [1,2,22] cannot be used in the present work. The numerical code was improved and the boundary condition at membrane surface was implemented to take on account the transmission of the solutes through the membrane. The procedure is described in the following paragraphs.

The mass boundary condition at the membrane surface, boundary VI, was established by performing a mass balance to a volume of fluid contiguous to the membrane surface. The volume of fluid and the respective pseudo-velocities along the normal direction, incoming $\hat{v}^m_{y_{up}}$, and, outgoing, $\hat{v}^m_{y_{down}}$, are represented in Fig. 1(A).

According to the finite volume method, the outcome of a mass balance to the control volume of Fig. A 1 is:

$$\frac{c^{k+1}_{g,1} - c^{k}_{g,1}}{\Delta t} = -\left(\frac{\hat{v}^m_{yu} c^{k+1}_{g,2} - \hat{v}^m_{yd} c^{k+1}_{g,1}}{\Delta y}\right) \tag{A.9}$$

where Δt is the time step, Δy the height of the node and the subscripts (g, 1) and (g, 2) refer to the node identification according to Fig. A 1.

The incoming pseudo-velocity to the node (g, 1), $\hat{v}^m_{yu}$ (Fig. A 1), is defined by the average between the pseudo-velocities at node (g, 1) and (g, 2):

$$\hat{v}^m_{yu} = \frac{\hat{v}_{y_{g,2}} + \hat{v}_{y_{g,1}}}{2} \tag{A.10}$$

The pseudo-velocity along the normal direction, leaving the discretized node (g, 1), $\hat{v}^m_{yd}$ (Fig. A 1), depends on the rejection coefficient ($R_{g,1}$) of the component and also on the pseudo-velocity at the node (g, 1).

$$\hat{v}^m_{yd} = \hat{v}_{y_{g,1}}(1 - R_{g,1}) \tag{A.11}$$

Since the osmotic pressure is negligible (diluted solution), the permeate velocity [23] through the membrane is given by:

$$-v_y = \frac{\Delta P_0}{\bar{\mu}_p R_m V_0} \tag{A.12}$$

where ΔP_0 is the applied pressure difference across the membrane. The pressure drop along the membrane was not taken on account (in previous studies [24], in identical flow conditions, this approximation has a maximum error of 5% in the flow field). R_m is the resistance of the membrane and $\bar{\mu}_p$ the viscosity of the permeate flux.

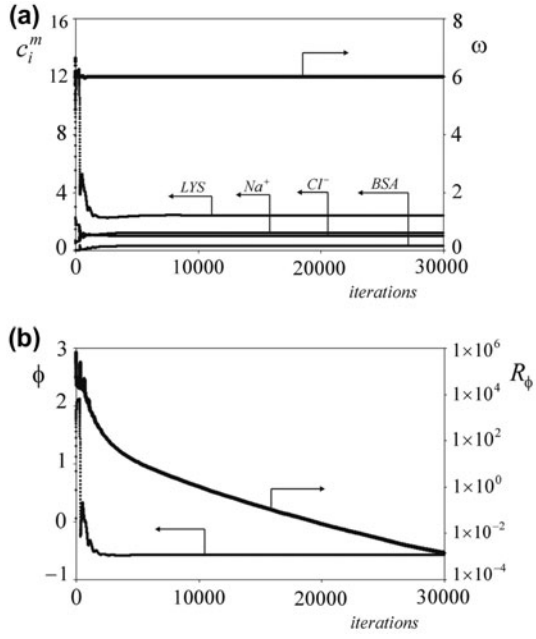

Fig. 1B. (a) Normalized concentration of the species and flow vorticity at the critical node versus the number of iterations; (b) Normalized electric potential and total residues of the electric potential equation at the critical node versus the number of iterations ($\mathrm{Re} = 95$, $Pe_{BSA} = 1.36 \times 10^6$, $Pe_{LYS} = 8.05 \times 10^5$, $Pe_{Na^+} = .14 \times 10^4$, $Pe_{Cl^-} = 4.68 \times 10^4$, $z_{BSA} = -21$; $z_{LYS} = +3$; $\Phi_w = -10mV(|z_{BSA} \times \Pi_3| = 8.119$ and $|z_{LYS} \times \Pi_3| = 1.160)$, $\Pi_1 = 1.07 \times 10^{-4}$, $\Pi_2 = 1.36 \times 10^5$, $\Pi_3 = 0.387$, $\Delta P_0 = 1 \times 10^4$Pa).

All the other conditions for boundary VI (Fig. 2) have been presented by Pinto et al. [1,2,22].

Appendix B

Convergence

The study of the convergence of the numerical method adopted was based on the following errors:

$$\varepsilon_{c_{i,crit}} = \left| \frac{c^{k}_{i,crit} - c^{k-1}_{i,crit}}{c^{k}_{i,crit}} \right| \tag{B.1}$$

$$\varepsilon_{\phi_{crit}} = \left| \frac{\phi^{k}_{crit} - \phi^{k-1}_{crit}}{\phi^{k}_{crit}} \right|; \tag{B.2}$$

$$\varepsilon_{\omega_{crit}} = \left| \frac{\omega^{k}_{crit} - \omega^{k-1}_{crit}}{\omega^{k}_{crit}} \right| \tag{B.3}$$

where *crit* refers to the critical node and k to the current iteration. The variables are evaluated in a critical node located near the cell exit, where the convergence is slower. More details about the iterative process are described by Pinto et al. [2].

The total sum of the residues of the electric potential equation, R_ϕ, was determined to assure that conservative equations converge to the correct solution:

$$R_\phi = \sum_{g=2}^{n-1} \sum_{h=2}^{m-1} \left| \frac{\partial \phi}{\partial t} \right|_{g,h} \tag{B.4}$$

where $\left|\frac{\partial \phi}{\partial t}\right|_{g,h}$ is the time derivative of the electric potential at node (g, h).

The following criteria were adopted to stop the iterative process:

$$\begin{cases} \varepsilon_{c_{i,crit}} < 10^{-3} \\ \varepsilon_{\phi_{crit}} < 10^{-3} \\ \varepsilon_{\omega_{crit}} < 10^{-3} \\ R_\phi < 10^{-2} \end{cases} \tag{B.5}$$

An example of the convergence of the numerical method, for the most severe conditions used (highest zeta-potential at the membrane surface), is presented in Fig. 1(B). The normalized concentrations, electric potential and vorticity converge to a constant value. The total residues of the Poisson–Boltzmann equation, R_φ, decreases to a very small value.